Petroleum 8 (2022) 167–173

Contents lists available at ScienceDirect

Petroleum

journal homepage: www.keaipublishing.com/en/journals/petlm

Predicting wax deposition using robust machine learning techniques

Menad Nait Amar [a, *], Ashkan Jahanbani Ghahfarokhi [b], Cuthbert Shang Wui Ng [b]

[a] Département Etudes Thermodynamiques, Division Laboratoires, Sonatrach, Avenue 1er Novembre, 35000, Boumerdes, Algeria
[b] Department of Geoscience and Petroleum, Norwegian University of Science and Technology, S. P. Andersens veg 15b, 7031, Trondheim, Norway

ARTICLE INFO

Article history:
Received 7 February 2021
Received in revised form
7 March 2021
Accepted 2 July 2021

Keywords:
Wax deposition
Multilayer perceptron
Levenberg-marquardt algorithm
Flow assurance

ABSTRACT

Accurate prediction of wax deposition is of vital interest in digitalized systems to avoid many issues that interrupt the flow assurance during production of hydrocarbon fluids. The present investigation aims at establishing rigorous intelligent schemes for predicting wax deposition under extensive production conditions. To do so, multilayer perceptron (MLP) optimized with Levenberg-Marquardt algorithm (MLP-LMA) and Bayesian Regularization algorithm (MLP-BR) were taught using 88 experimental measurements. These latter were described by some independent variables, namely temperature (in K), specific gravity, and compositions of C1–C3, C4–C7, C8–C15, C16–C22, C23–C29 and C30+. The obtained results showed that MLP-LMA achieved the best performance with an overall root mean square error of 0.2198 and a coefficient of determination (R^2) of 0.9971. The performance comparison revealed that MLP-LMA outperforms the prior approaches in the literature.

1. Introduction

Wax deposition is recognized as one of the severe problems that causes acute issues during the production of hydrocarbon fluids [1–3]. Wax deposition is mainly resulted from the precipitation of involved heavy paraffins in gas condensates and crude oils [4]. Many parts of the production systems, including surface facilities, risers, pipelines and separators, are exposed to this problem [1]. As the formation of wax occurs in any part of these systems, the efficiency of oil production is adversely impacted due to plugging caused by the deposited wax [5]. Severe economic loss will then follow because of reduced oil production. Hence, wax management has been one of the most important tasks in the petroleum industry for decades. Pertaining to this, there are different approaches that can be employed to mitigate the problem of wax deposition, such as pigging, thermal insulation, and injection of chemical [6–8]. However, applying these methods undeniably induces additional operating cost and it can be extravagant for the oil and gas companies to implement them without meticulous and proper planning. Due to this fact, it is necessary to determine accurately the parameters that characterize wax and help in the prediction of its deposition.

To have a better prediction of this problematic phenomenon, it is essential for us to understand the contributing factors or parameters that affect the deposition of wax. As Theyab [9] has counseled, these factors include temperature differential, cooling rate, flow rate, pressure, composition of crude oil, experimental time, and surface properties of pipe. Refer to the review discussed in Ref. [9] for the details. In general, wax deposition will take place when the conditions of reaching these affecting parameters are satisfied. From a thermodynamic perspective, these parameters can be explained by the change in the production conditions, profiles and the fluid composition [10]. In this context, various terminologies can be related to this mechanism, among which we can cite (1) wax appearance temperature (WAT), which is defined as the threshold temperature below which paraffin crystals are formed [3]; (2) wax disappearance temperature (WDT), which means the temperature at which the last deposited paraffin is removed; and (3) the amount of deposited was also known as the weight percent of deposited wax. The above-mentioned parameters are viewed as Solid–Liquid Equilibrium (SLE) descriptors, hence, their accurate determination is of vital role to extend the control of this phenomenon during the production.

* Corresponding author.
E-mail addresses: m.naitamar@univ-boumerdes.dz, manad1753@gmail.com (M. Nait Amar).
Peer review under responsibility of Southwest Petroleum University.

Production and Hosting by Elsevier on behalf of KeAi

https://doi.org/10.1016/j.petlm.2021.07.005

Direct measurements or experimental studies have been one of the methods employed to determine the SLE parameters. In this aspect, Dantes Neto et al. [11] used photoelectric signal and viscometry to find out the WAT in the systems of paraffin and solvent. Besides that, Jiang et al. [12] successfully determined the WAT of waxy oil under reservoir condition with the help of ultrasonic method. Mansourpoor et al. [13] also illustrated the use of viscometry and Differential Scanning Calorimetry (DSC) in determining the WAT of 12 Iranian oil and condensates samples. Regarding this, Chen et al. [14] also applied the DCS analysis to determine the wax content of crude oil. Furthermore, Wang et al. [15] investigated the nucleation processes and the impact of emulsification properties during the formation of waxy crude oil emulsion gels. In addition to this, Saxena et al. [16] employed proton Nuclear Magnetic Resonance (^{1}H NMR) to measure the wax content of crude oil. Some other equipment, such as cold finger, flow loop, and pour point tester can be of great interest for assessing the main descriptive parameters related with wax deposition. Peruse the review works done in Refs. [17,18] for more comprehensive discussion about the involvement of experimental studies in wax characterization. Despite being extensively employed, the experimental approaches generally incur expensive costs. Therefore, various thermodynamic models were proposed to study and predict the parameters of SLE. Ideal solid solution [19], multi-pure-solid [20], and Countinho's UNIQUAC [21] are among the leading paradigms in this field. However, although the simple conception of these models, several studies showed that some of the aforementioned models may fail in the estimation of the discussed parameters [1,22].

Due to this fact, a new kind of robust modeling techniques based on artificial intelligent (AI) methods is increasingly getting attention in the oil industry (including the prediction of flow assurance related phenomena) due to their notable prediction abilities [23–27]. Several literatures have highlighted the implementation of AI methods to predict the parameters of SLE. Regarding the prediction of WAT, Benamara et al. [3] modeled WAT using artificial neural network (ANN) and gene expression programming (GEP). Besides that, estimating WDT using AI approaches has also been another domain of discussion articulated in some literatures. In this case, Benamara et al. [1] applied radial basis function neural network (RBFNN) to predict WDT. They even coupled the RBFNN with two different metaheuristic algorithms, namely genetic algorithm (GA) and artificial bee colony (ABC) to perform the prediction. Bian et al. [28] established a WDT predictive model using support vector regression (SVR). The SVR model in Ref. [28] was also coupled with a metaheuristic algorithm that was grey wolf optimizer (GWO) and it showed very accurate predicted results. Furthermore, Obanijesu and Omidiora [29] built an ANN model that could forecast the potential of wax deposition of Nigeria crude oil. Chu et al. [30] implemented a hybrid model based on neuro fuzzy inference system (ANFIS) coupled with particle swarm optimization (PSO) for modeling wax deposition in oily systems. Gholami et al. [31] also established a committee machine (CM) by combining the results of amount of deposited wax estimated by SVR and ANN. The optimization of contribution of results by each of these two intelligent models was conducted by using GA. Additionally, Kamari et al. [5] developed a model for predicting the weight percent of deposited wax using least square support vector machine (LSSVM). In another investigation, Xie and Ying [32] also built a predictive model of wax deposition rate by applying RBFNN.

The aim of the present work is to establish new accurate predictive model for estimating the weight percent of deposited wax under different production conditions. To this end, two distinct models based on multilayer perceptron (MLP) optimized with Levenberg-Marquardt algorithm (MLP-LMA) and Bayesian Regularization algorithm (MLP-BR) were established using a comprehensive database. The obtained results from our models were compared with one of the best models in the literature, namely that developed by Kamari et al. [5].

The main novelty of the present study is the implementation of a rigorous type of grey-box machine learning techniques, namely MLP optimized with two robust algorithms, including LMA and BR for predicting the amount of deposited wax during the production. As a grey-box type, our best-developed model can be integrated in other related applications and commercial packages by mimicking its topology and its associated control parameters, such as weights and bias of the network.

2. Methodology

2.1. Multilayer perceptron (MLP)

Multilayer perceptron (MLP) is one of the robust types of artificial neural network (ANN). MLP is recognized with its high prediction ability when modeling many complicated systems with different degrees of complexity [33,34]. The remarkable performance of MLP can be explained by their flexible structure and the manner of treating the information during the learning process [35]. An MLP model covers three kind of layers: an input layer from where the inputs are introduced, one or more hidden layers which play an important role during the learning; and an output layer from which the modeling results are delivered. The hidden layers are characterized with their activation functions which allow the mapping of the inputs in higher dimensional spaces; and their number of neurons which differ according to the complexity of the studied phenomenon. The neurons of each layer are connected to the ones from the next layer by means of weights.

The learning phase of MLP aims at finding the proper weight values in order to minimized the error between the predictions and the real measurements. In this study, we have applied Levenberg-Marquardt algorithm (MLP-LMA) and Bayesian Regularization algorithm (MLP-BR) during the learning phase of MLP. More details about these algorithms can be found in published literature [35,36].

2.2. Data preparation

A comprehensive experimental database was considered for establishing the proposed models. This database include 88 experimental points [5]. These latter were reported in the published literature [37–39]. The reported data was gained using some experimental approaches, such as Pulsed NMR and Differential Scanning Calorimetry. The investigated output is the weight percent (wt %) of wax deposition at a pressure of 1 bar, while the considered input parameters correspond to temperature (in K), specific gravity (SP.GR), compositions of C1–C3, C4–C7, C8–C15, C16–C22, C23–C29 and C30+. Table 1 reports a statistical summary of the collected database.

2.3. Computational procedure

The gathered experimental measurements were normalized between −1 and 1 using the following expression:

$$X_n = \frac{2(X_i - X_{min})}{(X_{max} - x_{min})} - 1 \quad (1)$$

where X_n points out the normalized value of X_i, X_{max} *and* X_{min} represents the maximum and minimum values of *X,* respectively.

Afterwards, the database was divided into training (80% of the points) and testing (the remaining 20%) sets. Trial and error method was used to investigate the proper structure of the models.

Table 1
A statistical summary of the collected database.

	C1–C3	C4–C7	C8–C15	C16–C22	C23–C29	C30+	SP.GR	T (K)	Deposited Wax (wt %)
Min	0.218	3.057	33.468	16.029	0	0	0.872	230	0
Max	2.127	30.952	49.791	57.335	10	13.23	0.963	314.15	13
Avg.	1.316	18.477	44.496	29.005	2.812	3.539	0.919	272.66	3.142

3. Results and discussions

Before highlighting the main findings of our modeling approach, it is worth mentioning that trial and error method was carried out to investigate the proper number of hidden layers, their numbers of evolved neurons, and the suitable transfer functions. The best resulted MLP models trained with LM and BR algorithms contain three hidden layers, in each of them, Tansig is the proper activation function. The numbers of included neurons in each hidden layer are as follows: 11, 11, and 9 for the first, second and third hidden layer, respectively.

To assess the prediction performance of the established models, we have considered both statistical and graphical error analysis. The statistical evaluation was done using the following criteria:

Coefficient of Determination (R^2)

$$R^2 = 1 - \frac{\sum_{i=1}^{n}\left(Y_{iexp} - Y_{ipred}\right)^2}{\sum_{i=1}^{n}\left(Y_{ipred} - \overline{Y}\right)^2} \quad (2)$$

Root Mean Square Error (RMSE)

$$RMSE = \sqrt{\frac{1}{n}\sum_{i=1}^{n}\left(Y_{iexp} - Y_{ipred}\right)^2} \quad (3)$$

where Y_i represents the weight percent of deposited wax, subscripts *exp* and *pred* means the experimental and predicted Y values, respectively, $\overline{Y}$ is the average, and n is the number of data points.

Fig. 1 shows cross plots of the established MLP models, namely MLP-LMA and MLP-BR. According to this figure, it can be seen that the predictions of the implemented models are in good agreement with the real measurements of weight percent of deposited wax. For a detailed analysis of the performance of the newly proposed paradigms, Table 2 reports the statistical evaluation of these latter. As can be seen, MLP-LMA outperform MLP-BR with an overall RMSE value of 0.2198. Therefore, this model was kept for further analyses in this study.

To extend the examination of the reliability, some other graphical assessment techniques were applied on the implemented MLP-LMA model. Fig. 2 illustrates the distribution of the errors achieved by MLP-LMA model in all of the considered points during the training and testing phases. The plotted errors correspond to the difference between the real and predicted amounts of deposited wax. As can be seen, a satisfactory distribution of the errors associated with the MLP-LMA predictions is noticed near the zero-error line. In another evaluation, Fig. 3 depicts the cumulative frequency diagram of the absolute error related to the predictions of MLP-LMA paradigm. According to this diagram, it can be deduced that 90% of the data points can be estimated by our best-model with a small absolute error of 0.4%. Figs. 2 and 3 confirms again the noticeable integrity of the MLP-LMA paradigm while predicting the weight percent of deposited wax under different operating conditions.

A trend analysis was performed to testify if MLP-LMA model can follow the trend of weight percent of deposited wax (%) as function of temperature. The obtained results are shown in subplots a-c of Fig. 4 for three different samples. Besides, Table 3 states the main properties of these three samples. As can be seen, the predictions of MLP-LMA model are in excellent correspondence with the measured values for different temperature values. Besides, it can be observed that once the temperature of the systems falls significantly below WAT (in the subplots of Fig. 4, the WAT values correspond to the temperature values at which the deposition of wax begins, i.e. the first value with wt % > 0%), the amount of deposited wax increases generally as the decrease in temperature favors wax to crystallize from the oil [40–43]. However, it is worth mentioning that in some cases, the amount of deposited wax can initially increase, then decrease [44].

Lastly, our best established model (MLP-LMA) was compared with one of the best prior models, namely that proposed by Kamari et al. [5]. The comparison was done using the above-mentioned statistical criteria. Table 4 states the comparison results. According to the reported results in this table, it can be said that MLP-LMA outperforms Kamari et al. [5] model.

4. Conclusions

In the present investigation, two MLP models were developed based on LMA and BR algorithms to estimate the weight percent of deposited wax under different production conditions. The proposed

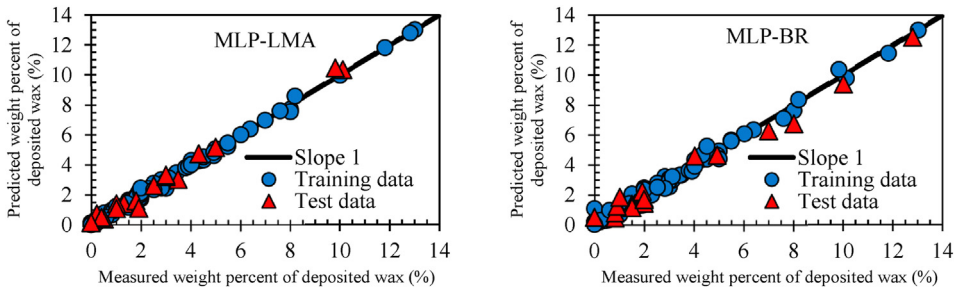

Fig. 1. Cross plots of the established MLP models for diffusion weight percent of deposited wax.

Table 2
Performance evaluation of the established MLP models.

		MLP-LMA	MLP-BR
Training	RMSE	0.1840	0.2967
	R^2	0.9982	0.9947
Test	RMSE	0.3589	0.5178
	R^2	0.9944	0.9914
All	RMSE	0.2198	0.3420
	R^2	0.9974	0.9940

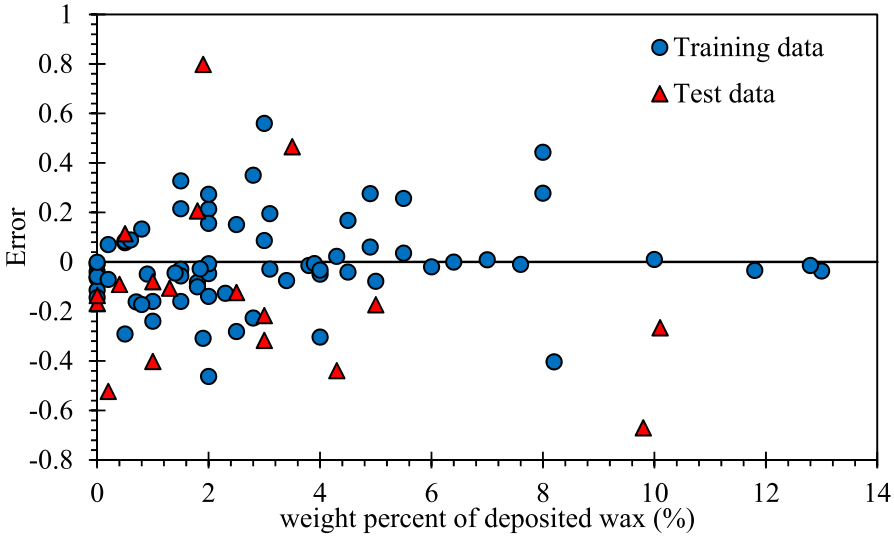

Fig. 2. Error distribution plot for the proposed MLP-LMA model.

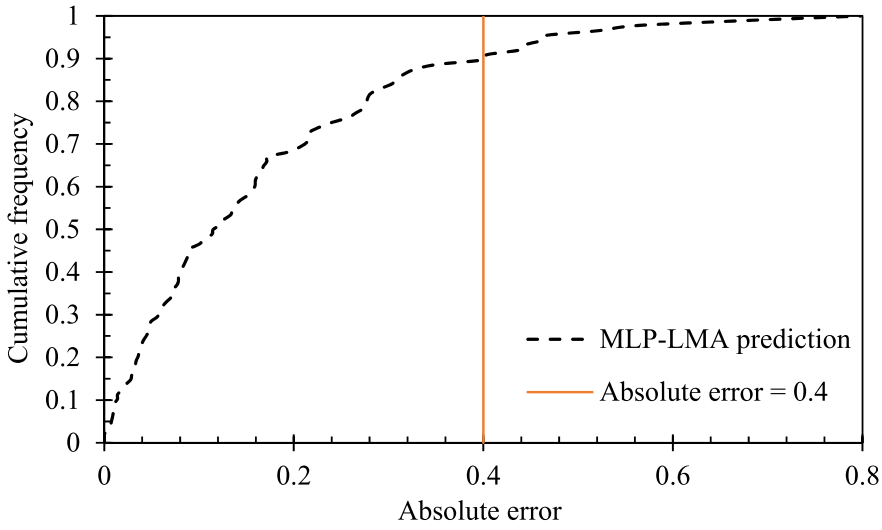

Fig. 3. Cumulative frequency diagram of the absolute error for the proposed MLP-LMA model.

models showed very satisfactory performance, while MLP-LMA was deemed superior to both MLP-BR and Kamari et al. models. MLP-LMA exhibited an overall RMSE value of 0.2198. The newly established model can contribute in many production systems to detect the amount of deposited was under different production conditions. Finally, as the MLP-LMA model can be transformed into an explicit expression (by taking the proper found weight values as shown in Appendix. A), this model can be implemented in digitalized system to improve the control of wax deposition.

Declaration of competing interests

The authors declare that they have no known competing financial interests or personal relationships that could have appeared to influence the work reported in this paper.

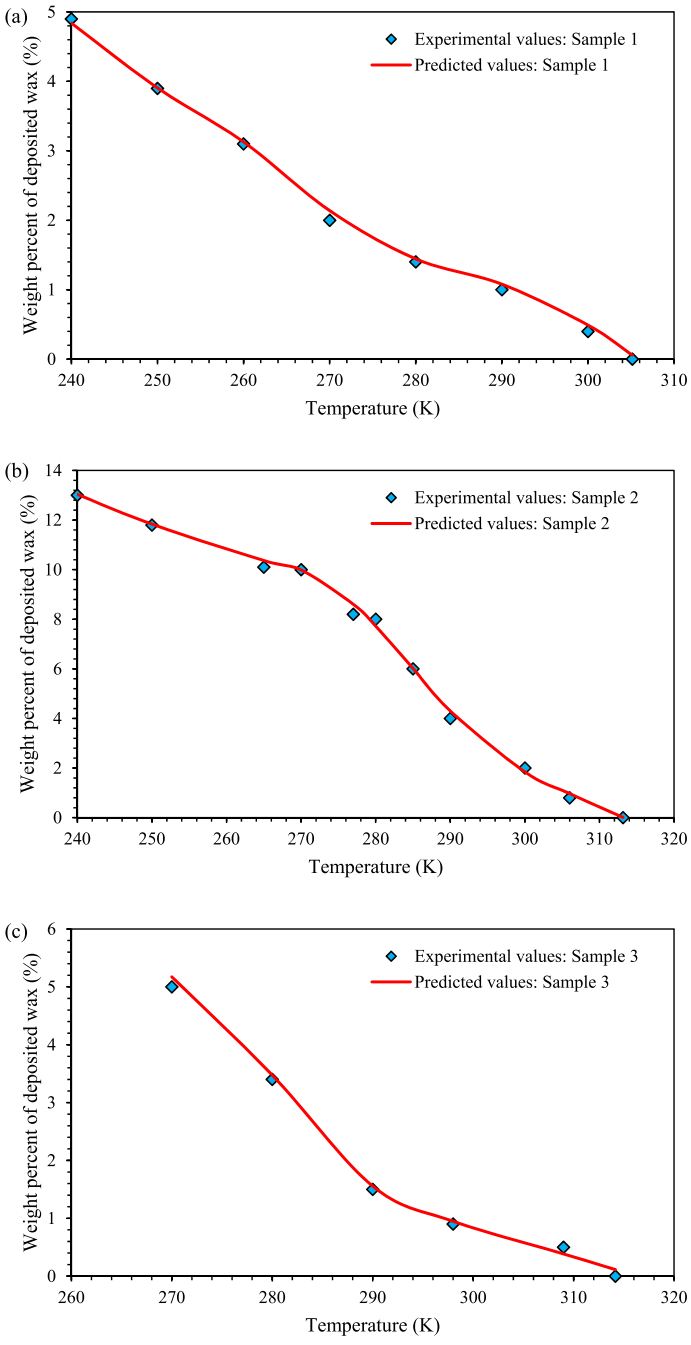

Fig. 4. Trend analysis.

Table 3
Properties of the three samples considered in the trend analysis.

	C1–C3	C4–C7	C8–C15	C16–C22	C23–C29	C30+	SP.GR
Sample 1	1.778	30.952	47.03	20.183	0	0	0.872
Sample 2	1.595	13.096	33.468	51.534	0	0	0.893
Sample 3	1.553	29.59	45.246	24.108	0	0	0.88

Table 4
Performance comparison.

	RMSE	R^2
MLP-LMA	0.2198	0.9974
Kamari et al. [5]	0.32	0.989

Appendix A

Table A.1
The main control parameters of the our best-implemented model (MLP-LMA)

Neurons	Weight values of connections between the input layer and the first hidden layer									
1	−0.1214	−0.7935	−0.3627	−1.0351	1.4440	2.0783	−0.2775	1.4533		
2	0.6609	0.5975	0.3440	1.7943	−0.0103	−1.3599	−0.0461	−1.9975		
3	0.6688	0.9695	0.2183	−0.4358	−0.1012	−1.1552	0.4860	1.5155		
4	0.2662	−0.2106	0.0404	1.0236	0.3581	−0.0534	−0.0328	−3.2874		
5	1.2762	−0.1689	0.7062	1.5947	0.2833	−0.6174	−0.6830	1.0171		
6	−0.9120	−0.4208	1.3372	−0.3453	−0.5025	0.8163	1.4224	−0.3890		
7	−1.5168	−1.5450	−0.5102	−0.0054	−1.1530	−0.7092	0.3792	−0.1601		
8	1.4824	0.5366	−0.4177	0.3972	0.0815	1.4090	1.0723	−0.0860		
9	1.1732	0.8334	0.3609	−1.2791	0.2466	−0.3886	0.9322	−0.6190		
10	−0.8071	0.1291	0.2619	0.7442	−0.4795	0.9668	1.2444	−0.3287		
11	1.3875	0.4443	−0.8075	−0.6100	0.6461	−0.5918	−1.1210	−0.6522		
Bias terms of the first hidden layer										
0.6953	−0.3310	−0.9787	−1.7627	−0.6242	0.9180	0.7564	−0.9147	0.9480	−2.0770	1.5620
Neurons	Weight values of connections between the first and second hidden layers									
1	0.3829	0.8408	−0.1083	1.4572	−0.5591	0.7641	−0.1911	0.7094	−0.8279	0.4351
2	0.6321	0.5957	0.6752	0.5062	0.1669	−0.6181	−0.2281	0.5931	−0.5619	0.3920
3	−0.3877	−1.2796	0.7158	0.2388	−0.0266	0.4227	−0.1846	−0.1184	1.2166	−0.3854
4	0.4237	−0.9387	0.3096	−0.3533	0.1224	−0.8354	−0.2425	−1.2610	−0.7577	0.3340
5	−0.0459	−1.3333	−0.2203	0.0125	1.1403	0.0148	−0.8348	−0.7273	−0.7961	−0.9085
6	−0.6766	0.4687	1.4289	−1.4857	0.1003	−0.2032	−0.4281	−0.9322	−0.4617	−0.0834
7	1.4952	−0.8383	−0.1024	−0.9197	−1.0372	1.3168	1.0521	1.0569	0.2789	−0.6061
8	−0.0410	−0.1225	0.6522	−0.8638	0.9254	0.3953	−0.6003	0.0989	−0.4896	−0.1573
9	−0.7697	0.8000	0.1846	−0.0007	−1.0467	−0.7395	−0.6051	−0.6789	−0.4604	−0.1867
10	0.2688	−0.5839	0.2236	−1.6047	−1.7157	−1.9485	−0.1589	−0.4583	−1.7549	−0.3709
11	−0.4181	0.0036	0.4732	0.9965	0.0625	0.1145	0.7338	0.6856	−0.7725	0.3370
Bias terms of the second hidden layer										
−1.6721	−1.3771	1.3076	−1.1178	−0.6449	−0.0681	0.6274	−1.3515	−1.2979	1.1520	−1.8261
Neurons	Weight values of connections between the second and third hidden layers									
1	0.7388	−0.4607	0.7969	−0.0310	−0.4606	0.5422	−0.1570	0.2270	0.9858	−0.5638
2	−0.9902	−0.6687	0.0948	0.4541	1.0639	0.5418	0.8991	0.8121	−0.2644	0.5763
3	0.5900	0.3975	0.7154	0.1798	0.5994	−0.0687	0.5279	−0.0035	0.6780	−0.9412
4	0.0100	0.0448	1.0183	−0.4257	0.6855	0.4583	−0.2671	−0.8440	−0.8323	−0.3671
5	−0.0810	−0.0403	−0.7112	0.1446	−0.1155	0.9299	−0.1762	−0.1470	0.0012	−0.6535
6	1.0286	1.0525	−0.5007	0.6508	0.3176	0.5069	0.3146	0.4810	−0.2330	−0.2308
7	0.4502	0.5403	0.1055	0.5745	1.4392	−0.1121	0.1431	0.0383	1.3192	1.8207
8	0.6118	0.2054	−1.5423	−0.7277	−1.0007	−0.6809	−0.9584	0.0675	−0.7194	−0.0757
9	−0.3295	0.2517	0.5186	1.3445	0.6233	0.4833	0.0277	0.9035	0.0195	−0.2006
Bias terms of the third hidden layer										
−2.0410	1.0622	−1.0964	−0.4074	−0.2095	0.0925	0.5220	1.4944	−2.0117		
Weight values of connections between the third hidden layer and the output layer										
0.1502	−0.8264	−0.4557	1.1625	0.6109	−0.1344	0.0226	1.0628	−0.3375	0.1502	
Bias term of the output layer										
−0.48574										
Transfer function of each of the hidden layers: Tansig										
Transfer function of the output layer: Pureline										

References

[1] C. Benamara, M. Nait Amar, K. Gharbi, B. Hamada, Modeling wax disappearance temperature using advanced intelligent frameworks, Energy Fuels 33 (2019) 10959–10968, https://doi.org/10.1021/acs.energyfuels.9b03296.

[2] A.M. Elsharkawy, T.A. Al-Sahhaf, M.A. Fahim, Wax deposition from Middle East crudes, Fuel 79 (2000) 1047–1055, https://doi.org/10.1016/S0016-2361(99)00235-5.

[3] C. Benamara, K. Gharbi, M. Nait Amar, B. Hamada, Prediction of wax appearance temperature using artificial intelligent techniques, Arabian J. Sci. Eng. 45 (2020) 1319–1330, https://doi.org/10.1007/s13369-019-04290-y.

[4] H.Y. Ji, B. Tohidi, A. Danesh, A.C. Todd, Wax phase equilibria: developing a thermodynamic model using a systematic approach, Fluid Phase Equil. 216 (2004) 201–217, https://doi.org/10.1016/j.fluid.2003.05.011.

[5] A. Kamari, A. Khaksar-Manshad, F. Gharagheizi, A.H. Mohammadi, S. Ashoori, Robust model for the determination of wax deposition in oil systems, Ind. Eng. Chem. Res. 52 (2013) 15664–15672.

[6] M.J. Jalalnezhad, V. Kamali, Development of an intelligent model for wax deposition in oil pipeline, J. Pet. Explor. Prod. Technol. 6 (2016) 129–133, https://doi.org/10.1007/s13202-015-0160-3.

[7] E. Bell, Y. Lu, N. Daraboina, C. Sarica, Experimental Investigation of active heating in removal of wax deposits, J. Petrol. Sci. Eng. 200 (2021) 108346.

[8] Z. Wang, J. Li, H.-Q. Zhang, Y. Liu, W. Li, Treatment on oil/water gel deposition behavior in non-heating gathering and transporting process with polymer flooding wells, Environ. Earth Sci. 76 (2017) 326.

[9] M.A. Theyab, Wax deposition process: mechanisms, affecting factors and mitigation methods, Open Access J. Sci. 2 (2018), https://doi.org/10.15406/oajs.2018.02.00054.

[10] M. del C. Garcia, L. Carbognani, Asphaltene- paraffin structural interactions. Effect on crude oil stability, Energy Fuels 15 (2001) 1021–1027.

[11] D. Neto, B. Neto, Determination of wax appearance temperature (wat) in paraffin/solvent systems by photoelectric signal and viscosimetry a, Brazilian J. Pet. Gas. 3 (4) (2009).

[12] B. Jiang, L. Qiu, X. Li, S. Yang, K. Li, H. Chen, Measurement of the wax appearance temperature of waxy oil under the reservoir condition with ultrasonic method, Petrol. Explor. Dev. 41 (2014) 509–512, https://doi.org/10.1016/S1876-3804(14)60059-8.

[13] M. Mansourpoor, R. Azin, S. Osfouri, A.A. Izadpanah, Experimental measurement and modeling study for estimation of wax disappearance temperature, J. Dispersion Sci. Technol. 40 (2019) 161–170, https://doi.org/10.1080/01932691.2018.1461635.

[14] J. Chen, J. Zhang, H. Li, Determining the wax content of crude oils by using differential scanning calorimetry, Thermochim. Acta 410 (2004) 23–26, https://doi.org/10.1016/S0040-6031(03)00367-8.

[15] Z. Wang, Y. Bai, H. Zhang, Y. Liu, Investigation on gelation nucleation kinetics of waxy crude oil emulsions by their thermal behavior, J. Petrol. Sci. Eng. 181 (2019) 106230.

[16] H. Saxena, A. Majhi, B. Behera, Prediction of wax content in crude oil and petroleum fraction by proton NMR, Petrol. Sci. Technol. 37 (2019) 226–233, https://doi.org/10.1080/10916466.2018.1536713.

[17] M.M. El-Dalatony, B.H. Jeon, E.S. Salama, M. Eraky, W.B. Kim, J. Wang, T. Ahn, Occurrence and characterization of paraffin wax formed in developing wells and pipelines, Energies 12 (2019), https://doi.org/10.3390/en12060967.
[18] F. Alnaimat, M. Ziauddin, Wax deposition and prediction in petroleum pipelines, J. Petrol. Sci. Eng. 184 (2020), https://doi.org/10.1016/j.petrol.2019.106385.
[19] J.H. Hansen, A. Fredenslund, K.S. Pedersen, H.P. Rønningsen, A thermodynamic model for predicting wax formation in crude oils, AIChE J. 34 (1988) 1937–1942, https://doi.org/10.1002/aic.690341202.
[20] C. Lira-Galeana, A. Firoozabadi, J.M. Prausnitz, Thermodynamics of wax precipitation in petroleum mixtures, AIChE J. 42 (1996) 239–248, https://doi.org/10.1002/aic.690420120.
[21] J.A.P. Coutinho, Predictive UNIQUAC: a new model for the description of multiphase solid-liquid equilibria in complex hydrocarbon mixtures, Ind. Eng. Chem. Res. 37 (1998) 4870–4875, https://doi.org/10.1021/ie980340h.
[22] A. Kamari, A. Khaksar-Manshad, F. Gharagheizi, A.H. Mohammadi, S. Ashoori, Robust model for the determination of wax deposition in oil systems, Ind. Eng. Chem. Res. (2013) 15664–15672, https://doi.org/10.1021/ie402462q.
[23] M. Nait Amar, Prediction of hydrate formation temperature using gene expression programming, J. Nat. Gas Sci. Eng. 89 (2021) 103879, https://doi.org/10.1016/j.jngse.2021.103879.
[24] M. Nait Amar, Modeling solubility of sulfur in pure hydrogen sulfide and sour gas mixtures using rigorous machine learning methods, Int. J. Hydrogen Energy 45 (2020) 33274–33287, https://doi.org/10.1016/j.ijhydene.2020.09.145.
[25] M. Nait Amar, M.A. Ghriga, H. Ouaer, On the evaluation of solubility of hydrogen sulfide in ionic liquids using advanced committee machine intelligent systems, J. Taiwan Inst. Chem. Eng. 118 (2021) 159–168, https://doi.org/10.1016/j.jtice.2021.01.007.
[26] A. Hemmati-Sarapardeh, R. Alipour-Yeganeh-Marand, A. Naseri, A. Safiabadi, F. Gharagheizi, P. Ilani-Kashkouli, A.H. Mohammadi, Asphaltene precipitation due to natural depletion of reservoir: determination using a SARA fraction based intelligent model, Fluid Phase Equil. 354 (2013) 177–184.
[27] A. Hemmati-Sarapardeh, B. Dabir, M. Ahmadi, A.H. Mohammadi, M.M. Husein, Modelling asphaltene precipitation titration data: a committee of machines and a group method of data handling, Can. J. Chem. Eng. 97 (2019) 431–441.
[28] X.Q. Bian, J.H. Huang, Y. Wang, Y.B. Liu, D.T. Kaushika Kasthuriarachchi, L.J. Huang, Prediction of wax disappearance temperature by intelligent models, Energy Fuels 33 (2019) 2934–2949, https://doi.org/10.1021/acs.energyfuels.8b04286.
[29] E.O. Obanijesu, E.O. Omidiora, Artificial neural network's prediction of wax deposition potential of Nigerian crude oil for pipeline safety, Petrol. Sci. Technol. 26 (2008) 1977–1991, https://doi.org/10.1080/10916460701399485.
[30] Z.Q. Chu, J. Sasanipour, M. Saeedi, A. Baghban, H. Mansoori, Modeling of wax deposition produced in the pipelines using PSO-ANFIS approach, Petrol. Sci. Technol. 35 (2017) 1974–1981, https://doi.org/10.1080/10916466.2017.1374405.
[31] A. Gholami, H.R. Ansari, S. Ahmadi, Combining of intelligent models through committee machine for estimation of wax deposition, J. Chin. Chem. Soc. 65 (2018) 925–931, https://doi.org/10.1002/jccs.201700329.
[32] Y. Xie, Y. Xing, A prediction method for the wax deposition rate based on a radial basis function neural network, Petroleum 3 (2017) 237–241, https://doi.org/10.1016/j.petlm.2016.08.003.
[33] A. Hemmati-Sarapardeh, A. Varamesh, M.M. Husein, K. Karan, On the evaluation of the viscosity of nanofluid systems: modeling and data assessment, Renew. Sustain. Energy Rev. 81 (2018) 313–329.
[34] M. Nait Amar, N. Zeraibi, K. Redouane, Bottom hole pressure estimation using hybridization neural networks and grey wolves optimization, Petroleum 4 (2018) 419–429, https://doi.org/10.1016/j.petlm.2018.03.013.
[35] S. Haykin, Neural Networks and Learning Machines, third ed., Pearson, Upper Saddle River, NJ, USA, 2001 https://doi.org/10.1002/1521-3773(20010316)40:6<9823::AID-ANIE9823>3.3.CO;2-C.
[36] A. Hemmati-Sarapardeh, M. Nait Amar, M.R. Soltanian, Z. Dai, X. Zhang, Modeling CO2 solubility in water at high pressure and temperature conditions, Energy Fuels 34 (2020) 4761–4776, https://doi.org/10.1021/acs.energyfuels.0c00114.
[37] W. Batsberg Pedersen, A. Baltzer Hansen, E. Larsen, A.B. Nielsen, H.P. Roenningsen, Wax precipitation from North Sea crude oils. 2. Solid-phase content as function of temperature determined by pulsed NMR, Energy Fuels 5 (1991) 908–913.
[38] K. Schou Pedersen, P. Skovborg, H.P. Roenningsen, Wax precipitation from North Sea crude oils. 4. Thermodynamic modeling, Energy Fuels 5 (1991) 924–932.
[39] A. Baltzer Hansen, E. Larsen, W. Batsberg Pedersen, A.B. Nielsen, H.P. Roenningsen, Wax precipitation from North Sea crude oils. 3. Precipitation and dissolution of wax studied by differential scanning calorimetry, Energy Fuels 5 (1991) 914–923.
[40] M. Lashkarbolooki, A. Seyfaee, F. Esmaeilzadeh, D. Mowla, Experimental investigation of wax deposition in Kermanshah crude oil through a monitored flow loop apparatus, Energy Fuels 24 (2010) 1234–1241.
[41] W. Wang, Q. Huang, C. Wang, S. Li, W. Qu, J. Zhao, M. He, Effect of operating conditions on wax deposition in a laboratory flow loop characterized with DSC technique, J. Therm. Anal. Calorim. 119 (2015) 471–485.
[42] S. Ravichandran, Mechanistic Study of Wax Deposition-Effect of Super Saturation, The University of Tulsa, 2018.
[43] A. Janamatti, Y. Lu, S. Ravichandran, C. Sarica, N. Daraboina, Influence of operating temperatures on long-duration wax deposition in flow lines, J. Petrol. Sci. Eng. 183 (2019) 106373.
[44] A. Dubey, Investigation of the Effects of Operating Conditions and Inhibitors on Paraffin Deposition, The University of Tulsa, 2016.